Available online at www.sciencedirect.com
SCIENCE DIRECT®
Journal of Molecular Catalysis A: Chemical 216 (2004) 101–106
JOURNAL OF MOLECULAR CATALYSIS A: CHEMICAL
www.elsevier.com/locate/molcata

Supported Re and Mo oxides prepared using binuclear precursors: synthesis and characterization

A.L. Kustov [a,*], V.G. Kessler [b], B.V. Romanovsky [a], G.A. Seisenbaeva [b], D.V. Drobot [c], P.A. Shcheglov [c]

[a] *Chemistry Department, M.V. Lomonosov State University, Moscow, Russia*
[b] *Chemistry Department, Swedish University of Agricultural Sciences, Upsala, Sweden*
[c] *M.V. Lomonosov State Academy of Fine Chemical Technology, Moscow, Russia*

Received 28 November 2003; received in revised form 28 November 2003; accepted 7 February 2004

Available online 9 April 2004

Abstract

Rhenium and molybdenum oxomethoxide complexes $Re_2O_3(OMe)_6$, $ReMoO_2(MeO)_7$, and $Mo_2O_2(OMe)_8$ were used as precursors to prepare highly dispersed mono and bimetallic oxide species supported on the microporous NaY zeolite and mesoporous SiO_2 and Al_2O_3. The prepared materials were characterized by the use of FTIR, NH_3-TPD, and H_2-TPR techniques. It was shown that, upon loading into microporous zeolite, oxomethoxide complexes loose their ligands so that just metal suboxide cores remains in the intracrystalline voids as the nanosized oxide clusters. The obtained clusters reveals both acidic and redox properties. The maximum amount of NH_3 adsorbed per bimetallic species could be used as a characteristic of both availability of acid sites and oxide dispersion. Reducibility of these species depends strongly on both their location in the matrix and the size. The matrix texture also affects the transitions between different valent states of Re and Mo as well as the metal reduction extent.

Keywords: Nanomaterials; Zeolites; Re and Mo oxides; Binuclear oxomethoxides; FT-IR; TPD-NH_3; TPR-H_2

1. Introduction

The properties of supported metal and metal oxide catalysts depend dramatically on the dispersion of an active moiety that is, in turn, dependent on the preparation conditions, and first of all on the nature of the precursor used. In the case of micro and mesoporous zeolites and other supports, the ion exchange and impregnation of the carrier with aqueous solutions of salts followed by thermal, oxidative, or reductive degradation of a precursor introduced are traditionally applied for the preparation of such catalytic materials. However, this preparation technique often requires higher temperatures; that is why the decomposition of the precursor compound is almost inevitably complicated by the migration and aggregation of metal or oxide particles, which deteriorates the efficiency of the catalyst. Even greater difficulties could arise during the preparation of the ultradisperse bimetallic particles because the segregation of the components leading to the chemical inhomogeneity, can also occur in this case.

These difficulties can be overcome by using organometallic or metal complex precursors with labile organic ligands. Such precursors are readily transformed into a metal or metal oxide phase under mild conditions [1–4]. In this respect, polynuclear mono and bimetallic oxomethoxide complexes are of particular interest [1]. The in situ thermal or redox decomposition of these precursors yields the polyatomic species—metal or metal oxide clusters—whose mobility is substantially hindered within the cages of the support. Besides, this synthesis affords metal or oxide nanoparticles with uniform composition that correspond to the metal-to-metal ratio in the starting compound.

In the present work, homo and heterometallic Re and Mo oxide clusters encapsulated inside the microporous Y zeolite and mesoporous SiO_2 and Al_2O_3 were prepared via in situ synthesis using binuclear oxomethoxide complexes as precursors. No attempts to use the heterobinuclear metal

* Corresponding author. Tel.: +7-95-9393570; fax: +7-95-9328846.
E-mail addresses: arkus@mail.ru (A.L. Kustov), vadim.kessler@kemi.slu.se (V.G. Kessler), p_shcheglov@mtu-net.ru (P.A. Shcheglov).

1381-1169/$ – see front matter © 2004 Elsevier B.V. All rights reserved.
doi:10.1016/j.molcata.2004.02.009

alkoxide complexes for the preparation of nanocomposite materials of this kind have been reported so far. Three major distinctive features of metal alkoxides as starting compounds are particularly attractive. First, they are well soluble in organic polar solvents. Second, their oxidation resulting in the corresponding bimetallic oxides occurs at rather low temperatures [5]. Third, the molecular dimensions of these complexes can be readily adjusted to the steric requirements of in situ synthesis by varying the size of alkoxide ligands.

On the other hand, the Re and Mo containing materials could be of both academic and practical interest as the catalysts for a wide variety of organic reactions.

2. Experimental

Re–Mo oxomethoxide complexes, were obtained by anodic oxidation of metal Re and Mo. Details of this synthetic approach were described elsewhere [5–8]. The composition and structure of prepared $Re_2O_3(OMe)_6$ [9,10], $ReMoO_2(OMe)_7$ [6], and $Mo_2O_2(MeO)_8$ [8] complexes were characterized using the chemical microanalysis, X-ray single crystal and powder diffraction techniques, MS technique, IR and NMR spectroscopy.

Microporous NaY zeolite with the molar ratio $SiO_2/Al_2O_3 = 5.1$ and a surface area of 663 m^2/g was used as a starting matrix material. For comparison, mesoporous SiO_2 (110 m^2/g) and Al_2O_3 (210 m^2/g) were also applied as a supports. Prior to use, all these supports were calcined in air at 450 °C for 6 h.

Incipient wetness impregnation with methanol solutions was used to introduce Re–Mo precursors into the supports. Then, prepared samples were dried at room temperature. Unless otherwise indicated, the samples were calcined at 450 °C for 4 h in air. These homo and heteronuclear samples are denoted further as $M^1M^2O_6$/support (M^1 and M^2 means Re or Mo atoms). For comparison, ReO_3+NaY and MoO_3+NaY samples that represented the mechanical mixtures of NaY powder and individual Re or Mo oxides were also prepared.

The metal contents in these samples were determined by the atomic absorption spectroscopy technique and were found to be within the range 1–5 wt.%.

FT-IR spectra were recorded with a Nicolet Protege 460 spectrometer using the standard KBr technique.

Temperature-programmed desorption of ammonia (NH_3-TPD) was performed according to the following procedure: 150 mg of the sample was loaded into a quartz tube reactor and calcined at 400 °C in dry air flow (2 h, 30 ml/min) and then in dry nitrogen flow (2 h, 30 ml/min). After that the sample was cooled to the room temperature and was kept in a flow of dry NH_3 for 30 min. Then, the reactor with the sample was closed and left overnight. Before the NH_3 desorption measurement, the sample was heated to 100 °C in a dry helium flow and kept at this temperature for 1 h to remove physically-adsorbed ammonia. Then the sample was cooled to room temperature and the temperature was raised at a rate of 5 °C/min up to 800 °C. The rate of NH_3 desorption was monitored by a computer-interfaced thermal conductivity detector using the ECOCHROM software to collect and process TPD data. The total amount of desorbed NH_3 was evaluated as the area under the TPD curve.

Temperature-programmed reduction (TPR) was performed as follows: 200 mg of sample calcined at 450 °C for 5 h was loaded into a quartz tube reactor and then activated by heating at 200 °C in a flow of dry Ar (10 ml/min) for 2 h. After cooling to room temperature, the Ar flow was changed for the reducing gas mixture (3.5 vol.% H_2 in Ar, 25–30 ml/min), and the temperature was raised at a rate of 10 °C/min up to 1000 °C. The rate of hydrogen consumption was monitored by a computer-interfaced thermal conductivity detector using the ECOCHROM software to collect and process TPR data. The total amount of hydrogen consumed was evaluated as the area under a TPR curve.

3. Results and discussion

The structures of the starting binuclear complexes are shown in Fig. 1. Metal atoms in the binuclear complexes have a six-fold coordination to the oxygen atoms. In addition to the metal–metal bond they are connected via several bridging metoxy groups (except for $Mo_2^{VI}O_2(MeO)_8$ complex which has no Mo–Mo bond in its structure). Given this specificity of precursor structures, one could suppose that the complex core would remain intact in the course of various treatments so that the metal-to-metal ratio in the resulting oxides will be similar to that in the starting precursor species.

On the other hand, the major requirement for using one or another complex as a precursor in the preparation of zeolite-based nanocomposites is the geometric adequacy between the matrix pore size and complex molecule dimensions. So, we evaluated the dimensions of these binuclear oxomethoxide complexes using a standard quantum chemistry approach available in 'HyperChem' soft. The estimated values (in Å) are given as follows.

$Re_2O_3(OMe)_6$	$Mo_2O_2(MeO)_8$	$ReMoO_2(MeO)_7$
8.4 × 5.3	9.1 × 5.5	9.2 × 6.1

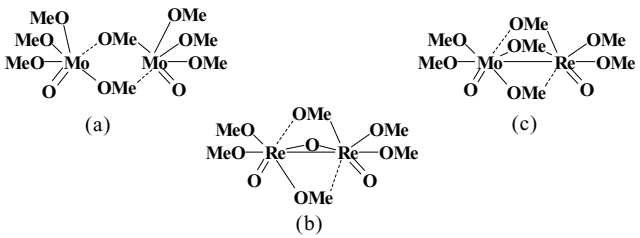

Fig. 1. Structures of binuclear oxomethoxide Re and Mo complexes: (a) $Mo_2O_2(MeO)_8$, (b) $Re_2O_3(OMe)_6$, (c) $ReMoO_2(MeO)_7$.

Table 1
Metal contents (wt.%) in Re- and Mo-containing samples

No.	Sample	Re	Mo	No.	Sample	Mo
1	Re_2O_6/NaY	4.24	–	5	Mo_2O_6/NaY	2.27
2	$ReMoO_6$/NaY	1.53	0.90	6	Mo_2O_6/SiO_2	2.15
3	$ReMoO_6/SiO_2$	1.01	2.97	7	Mo_2O_6/Al_2O_3	2.21
4	ReO_3 + NaY	5*		8	MoO_3+NaY	5*

* Calculated on the basis of the metal content in the starting chemicals.

From these data, one could suggest that the molecules of binuclear complexes might easily penetrate into the 8 Å-zeolite channels. Meanwhile, the presence of a single precursor molecule inside the Y zeolite large cage of 12 Å in diameter should make it difficult for the second molecule to accommodate within the same cavity. Therefore, one may expect that in situ oxidative treatment of the impregnated samples leads to the formation of both isolated oxide species with definite distribution among the zeolite matrix and bulk oxide species located on the outer surface of the zeolite support.

The contents of Re and Mo metals in prepared samples are given in Table 1. The atomic Re:Mo ratio in calcined $ReMoO_6$/NaY sample is quite similar to the atomic stoichiometry in the starting heterometallic precursors. At the same time, the significant decrease of this ratio was found in the case of silica-supported heterometallic oxide. This could be resulted from partial removal of Re during the calcination procedure, which was visually observed as the formation of deep-blue coating at the reactor outlet during the heating of the sample in air flow.

The results of IR-spectroscopy were rather unexpected because the spectra of freshly prepared Re_2O_6/NaY, Mo_2O_6/NaY and $ReMoO_6$/NaY samples were quite similar to the spectra of starting NaY and did not exhibit any characteristic bands of organic groups [11].

The same results were obtained by applying the DTA method to study the samples loaded with the oxomethoxide complexes. In fact, DTA profiles of freshly impregnated and air-dried samples did not show any exothermic peak that could be attributed to the combustion of the complex ligands or some organic residues. The absence of the exothermic peaks corresponding to the burning of organic molecules in these solvent-free samples indicates that the molecule of the complex on contacting with zeolite loses its methoxide ligands so that only oxide core penetrate into the mircoporous material. Apparently, the molecule of metal complex could be subjected to hydrolisis with residual water that presents on the zeolite support. It seems that this process could be enhanced by own Bronsted and Lewis acid sites of the zeolite support resulting in a specific replacement of methoxide ligands of the complex by oxygen atoms of the zeolite framework. The formation of suboxide species on contacting the complex molecule with zeolite material can be also resulted from some non-hydrolitic reactions such as elimination of ether or β-scission well known for Re and Mo compounds

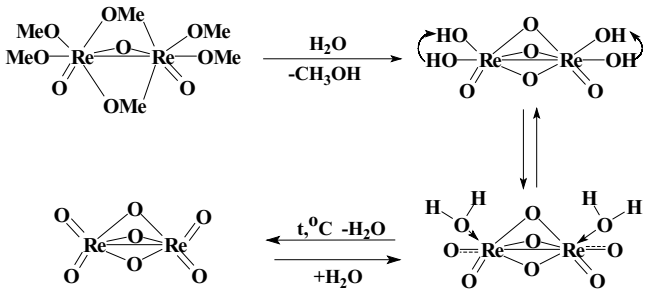

Fig. 2. Scheme of the decomposition of oxomethoxide complexes.

[12]. This process could be described by the scheme presented in Fig. 2.

Quite opposite situation is observed in the case of silica-supported samples, because mesoporous silica has much bigger pores then microporous zeolite and does not reveal any acidic properties. In this case the IR-spectra of SiO_2-supported $ReMoO_2(OMe)_7$ complex (freshly prepared and air-dried) reveals adsorption bands at 2800–3000 cm^{-1} characteristic to the organic groups of the oxomethoxide complex. These adsorption bands disappear after the calcination of the sample at 450 °C, indicating the formation of corresponding oxide.

In the mechanism presented on Fig. 2, the decomposition of the supported oxomethoxide complexes leads to the formation of corresponding bimetallic oxide species. It is known [13] that oxides of Re and Mo should exhibit acidic properties and therefore can bind several NH_3 molecules. Thus, the maximum number of adsorbed NH_3 molecules per metal pair would be characteristic of both availability of these acid sites and oxide dispersion.

This hypothesis was confirmed by the results of TPD-NH_3. The results of TPD-NH_3 measurements for supported Re and Mo bimetallic oxides as well as that of initial NaY are summarized in Table 2.

As it is seen from these data, all supported oxide samples contain weak acidic centers (the maximum on the TPD profile at ∼200 °C) similar to those present in the initial NaY zeolite. At the same time, the total acidity considerably changes on going from sample to sample. The acidity of the initial NaY support is most probably connected with the own Bronsted acid sites of the zeolite as well as

Table 2
TPD-NH_3 results for NaY and supported Re and Mo binuclear oxides

Sample	NaY	Mo_2O_6/NaY	Re_2O_6/NaY	$MoReO_6$/NaY
t_{max} (°C)	192	190	206	201
S (μmol/g[a])	618	584	707	967
$S - S^0$ (μmol/g[b])	–	(−34)	89	349
Me_2 content (μmol/g)	–	118	114	88
Molar NH_3/Me_2	–	–	0.78	3.97

[a] The total amount of desorbed NH_3 calculated from the area under the TPD-curve.

[b] Difference between the acidity of supported samples and initial NaY.

Table 3
TPD-NH_3 results for NaY and SiO_2 supported Re–Mo bimetallic oxides

Sample	$ReMoO_6$/NaY	$ReMoO_6/SiO_2$
t_{max} (°C)	201	218
NH_3 (μmol/g[a])	349	108
Molar NH_3/Me_2	3.97	2.01

[a] Difference between the acidity of supported samples and initial carrier.

sodium ions (Lewis acid sites) capable to hold ammonia. A small decrease in the total acidity of Mo_2O_6/NaY in comparison with NaY could be caused by the formation of molybdate-like compounds. The similar results for zeolite supported Mo oxide were observed earlier in [14]. The acidity of the Re_2O_6/NaY catalyst obtained using binuclear precursor is 25% higher and the ammonia desorption peak is shifted by 10 °C toward higher temperatures in comparison with the starting zeolite. The heterobimetallic $MoReO_6$/NaY catalyst exhibits the highest acidity, which is about 60% higher than that of the zeolite support. The decrease of the number of NH_3 molecules per bimetallic unit as calculated from TPD data could be resulted from two reasons: first, aggregation of isolated oxide molecules into larger particles and, second, different interactions of the binuclear complex with the support (anchoring or formation of molybdate or perrhenate compounds). Therefore, the maximum amount of NH_3 adsorbed per bimetallic unit would be characteristic of both availability of its acid sites and oxide dispersion.

From this viewpoint, it would be interesting to compare the date on ammonia TPD obtained for the samples prepared using different supports: microporous NaY and mesoporous SiO_2 (Table 3). In the case of silica having the pore size approximately ten times larger then NaY, the formation of quite large aggregated oxide particles should be expected. Besides that, nonacidic SiO_2 does not reveal any specific interaction with supported oxides and therefore the dispersion of forming bimetallic oxides would be considerably lower then in the case of NaY. Unfortunately, it is quite difficult to estimate the dispersion of Al_2O_3 supported samples using this technique, because of the substantial own acidity of this support.

On the other hand, there exists another possibility to estimate the dispersion of supported oxide species. As it was shown in [15–17] a reducibility of oxide particles is strongly affected by their size: the smaller oxide particle the higher is the temperature of reduction. So, we tried to apply TPR-H_2 technique for this estimation.

For all samples the TPR profiles of all samples studied exhibits several reduction peaks the temperatures and intensities of which depend on the nature of both metal and support as well as on the mode of preparation. Three reasons of these TPR patterns may be considered. First, the different accessibility of oxide species located at the outer surface of the support, in the channels and encapsulated within the cages may account for the multiple-peak TPR profiles. Second, the reduction of oxide particles of different size could

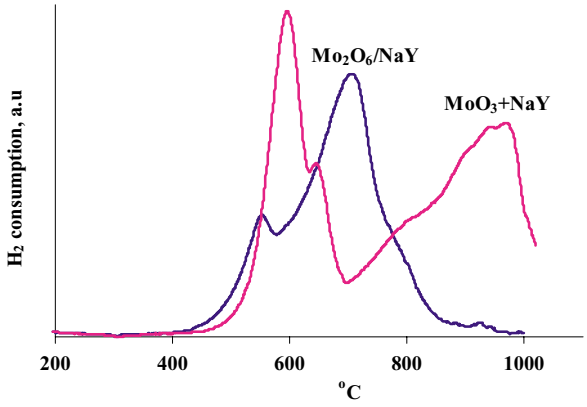

Fig. 3. Temperature-programmed reduction profiles of the $MoO_3 + NaY$ mixture and supported Mo_2O_6/NaY sample.

proceed at different temperatures. And third, the transitions between various oxidation states of Re and Mo atoms may occur in different temperature regions. The last explanation seems to be more plausible upon comparing the TPR patterns of zeolite-supported Mo oxides and of the mixtures of NaY + individual Mo oxide (Fig. 3). In fact, if we assume that two peaks on TPR curves of composite materials are the result of the reduction of oxide nanoclusters differently hosted in a matrix, then the free oxide should exhibits only one reduction peak because of equal accessibility of all oxide particles for oxidation. Meanwhile, the TPR profile of the $MoO_3 + NaY$ mechanical mixture exhibits, at least, two well-separated peaks. Nevertheless, the presence and relative intensities of the peaks on TPR profiles cannot be explained only by the transitions between different oxidation states of the metal. In fact, the ratio between low-temperature and high-temperature peak areas as estimated from TPR curves for the $NaY + MoO_3$ mixture (Fig. 3) is 2:3, whereas for the stepwise reduction Mo(VI) → Mo(IV) → Mo(0), the ratio should be 1:2. It has to be noted that the total area under this TPR curve is 2.95 H_2 molecule per Mo atom, which corresponds to the almost complete reduction of molybdenum oxide to the metallic state.

Effect of dispersion on the temperature of transitions between different oxidation states of the metal is revealed even more clearly in the case of Re-containing samples. The TPR curves obtained for rhenium oxide in the $ReO_3 + NaY$ mixture (large particles) and for supported Re_2O_6/NaY sample (nanoparticles) are presented in Fig. 4.

Several high temperature peaks are observed in the case of highly dispersed Re oxide clusters in NaY zeolite. Since the total amount of consumed hydrogen for both samples was approximately the same and corresponded to the complete reduction of Re oxide (about three H_2 molecules per Re atom), one could suggest that, unlike bulk rhenium oxide, the stabilization of various Re oxidation states takes place in the case of its clusters encapsulated inside the zeolite cages. This notion becomes rather reasonable if we take into account two facts: first, the larger the oxide particle

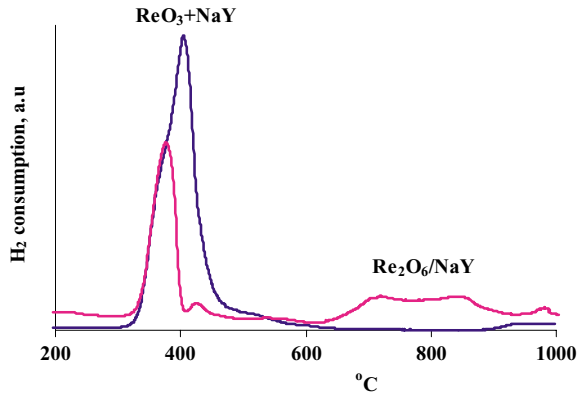

Fig. 4. TPR profiles of Re_2O_6/NaY and ReO_3 + NaY.

size, the easier its reduction, and, second, the aggregation of nanosized particles should precede their reduction [15,17]. So, the complete reduction of these nanoparticles would be achieved only at high enough temperatures close to those of the zeolite structure collapse. In the case of large microsized particles, the difference in temperatures of the transitions between different oxidation states is not so noticeable and the reduction peaks overlap; therefore, the TPR experiment reveals only one reduction peak that represents superposition of several peaks that are clearly seen in the TPR curves of nanosized Re oxide particles.

The texture of the matrix used influences both the reduction temperature and the completeness of oxide reduction. The reduction patterns of Mo oxide in the MoO_3 + NaY mixture and supported on silica, alumina, and zeolite supports are summarized in Table 4.

These data show that complete reduction of molybdenum oxide to the metal state occurs only in the case of bulk oxide with a poor dispersion as in the mechanical MoO_3 + NaY mixture. As to supported samples, the depth of the reduction noticeably decreases on decreasing the pore diameter and on increasing specific interactions between molybdenum oxide species and the support surface. Therefore, the reduction is minimal in the case of the microporous NaY matrix and does not exceed 60%.

If one accepts such an explanation, it would be possible to evaluate the relative oxide phase dispersion in the samples analogous in the chemical composition. This assumption was verified for the Mo_2O_6/NaY sample before and after extraction with an NH_4OH solution. This extraction results in a partial removal of molybdenum oxide (up to 50% according to the elemental analysis data). At the same time, the hydrogen uptake decreases two times from 2.37 to 1.19 mol H_2/atom Mo. It is quite evident that the extraction removes preferentially the molybdenum oxide material located at the outer surface of the support since the preparation method does not exclude the formation of large oxide particles out of the zeolite interior.

Table 4
Hydrogen consumption during the temperature-programmed reducton of samples

Sample	Molar H_2/metal	Pore diameter, Å
MoO_3 + NaY	2.95	–
Mo_2O_6/SiO_2	2.38	120
Mo_2O_6/Al_2O_3	2.12	150
Mo_2O_6/NaY	1.71	12

4. Conclusions

- Oxomethoxide binuclear Re and Mo complexes loose their ligands when loaded into the microporous NaY zeolite, so that just metal suboxide cores remains in the intracrystalline voids and reside there as the nanosized particles.
- Binuclear oxide species, obtained using oxomethoxide Re and Mo complexes, may bind up to four molecules of NH_3. The maximum amount of NH_3 adsorbed would be characteristic of both availability of acid sites and oxide dispersion.
- The decrease of the number of NH_3 molecules per bimetallic unit could be resulted from two reasons: first, aggregation of isolated oxide molecules and, second, different interactions of the binuclear complex with the support.
- The reduction of Re and Mo oxide nanoparticles is strongly influenced by the structure of the support. The temperature of the transitions between different reduction states of metals depends on their interraction with carrier and is characteristic of the oxide phase dispersity, the reduction of more dispersed particles requires higher temperatures.

Acknowledgements

This work was supported by Russian Foundation for Basis Research (Projects Nos. 01-03-32142 and 00-15-97346), by the Russian Presidential Foundation (Project No. 1275.2003.3) and Swedish Scientific Research Council. A.L. Kustov is grateful to HALDOR TOPSOE A/S for providing a Ph.D. student grant.

References

[1] R. Jelinek, S. Ozkar, G.A. Ozin, J. Phys. Chem. 96 (1992) 5049.
[2] T.M. Abdel-Fattah, G. Davies, in: C.A.C. Sequeira, M.J. Hudson (Eds.), Multifunctional Mesoporous Inorganic Solids, Kluwer Academic Publishers, Holland, 1993, p. 121.
[3] T.M. Abdel-Fattah, G. Davies, B.V. Romanovsky, O.L. Shakhnovskaya, A.M. Larin, S.A. Jansen, M.J. Palmieri, Catal. Today 89 (1996) 670.
[4] Y. Okamoto, H. Kikuta, Y. Ohto, S. Nasu, O. Terasaki, Stud. Surf. Sci. Catal. 105 (1997) 2051.
[5] K.G. Caulton, L.G. Hubert-Pfalzgraf, Chem. Rev. 90 (1994) 969.
[6] V.G. Kessler, G.A. Seisenbaeva, A.V. Shevelkov, G.V. Khvorykh, J. Chem. Soc., Chem. Commun. (1995) 1779.

[7] V.G. Kessler, G.A. Seisenbaeva, D.V. Drobot, Soft chemistry route to rhenium-based materials, in: B.D. Bryskin (Ed.), Rhenium and Rhenium Alloys, The Minerals, Metals & Materials Society, 1997, p. 167.
[8] V.G. Kessler, A.V. Mironov, N.Y. Turova, A.I. Yanovsky, Y.T. Struchkov, Polyhedron 12 (1993) 1573.
[9] P. Edwards, G. Wilkinson, Dalton Trans. (1984) 2695.
[10] G.A. Seisenbaeva, A.V. Shevelkov, L. Kloo, S. Gohil, J. Tegenfeldt, V.G. Kessler, Dalton Trans. 19 (2001) 2762.
[11] L.V. Vilkov, Y.A. Pentin, Physical Methods in Chemistry: Structure Characterisation and Optical Spectroscopy, Vyshaya Shkola, Moscow, 1987, p. 367.
[12] P.A. Shcheglov, D.V. Drobot, G.A. Seisenbaeva, S. Gohil, V.G. Kessler, Chem. Mater. 14 (2002) 2378.
[13] K. Tanabe, Solid Acids and Basis, Moscow, 1973, p. 157.
[14] L. Lietti, G. Ramis, G. Busca, F. Bregani, P. Forzatti, Catal. Today 61 (1–4) (2000) 187.
[15] P.A. Chernavskii, Catal. Lett. 45 (1997) 215.
[16] R. Thomas, E.M. Van Oers, V.H.J. de Beer, J. Medema, J.A. Moulijn, J. Catal. 76 (2) (1982) 241.
[17] P.A. Chernavsky, Doctor of Science Dissertation, MSU, Moscow, 2001.